AGU PUBLICATIONS

JGR

Journal of Geophysical Research: Space Physics

COMMENT

10.1002/2017JA024779

This article is a comment on Ngwira et al. (2014) http://doi.org/10.1002/2013JA019661.

Key Points:
- The densities used in Ngwira et al. (2014) are unnecessarily too high. Such densities are not needed
- It is shown that typical solar wind densities can be used to explain the Carrington storm features
- High solar wind densities are not needed to explain the Carrington storm short recovery phase. An alternate mechanism is given

Correspondence to:
B. T. Tsurutani,
bruce.t.tsurutani@jpl.nasa.gov

Citation:
Tsurutani, B. T., Lakhina, G. S., Echer, E., Hajra, R., Nayak, C., Mannucci, A. J., & Meng, X. (2018). Comment on "Modeling extreme "Carrington-type" space weather events using three-dimensional global MHD simulations" by C. M. Ngwira, A. Pulkkinen, M. M. Kuznetsova, and A. Glocer". *Journal of Geophysical Research: Space Physics*, *123*, 1388–1392. https://doi.org/10.1002/2017JA024779

Received 13 SEP 2017
Accepted 26 DEC 2017
Accepted article online 18 JAN 2018
Published online 26 FEB 2018

Comment on "Modeling Extreme "Carrington-Type" Space Weather Events Using Three-Dimensional Global MHD Simulations" by C. M. Ngwira, A. Pulkkinen, M. M. Kuznetsova, and A. Glocer"

Bruce T. Tsurutani[1], Gurbax S. Lakhina[2], Ezequiel Echer[3], Rajkumar Hajra[4], Chinmaya Nayak[5], Anthony J. Mannucci[1], and Xing Meng[1]

[1]Jet Propulsion Laboratory, California Institute of Technology, Pasadena, CA, USA, [2]Indian Institute of Geomagnetism, Navi Mumbai, India, [3]INPE, São José dos Campos, Brazil, [4]LPC2E, CNRS, Orléans, France, [5]Department of Physics and Astronomy, George Mason University, Fairfax, VA, USA

Abstract An alternative scenario to the Ngwira et al. (2014, https://doi.org/10.1002/2013JA019661) high sheath densities is proposed for modeling the Carrington magnetic storm. Typical slow solar wind densities (~5 cm^{-3}) and lower interplanetary magnetic cloud magnetic field intensities (~90 nT) can be used to explain the observed initial and main phase storm features. A second point is that the fast storm recovery may be explained by ring current losses due to electromagnetic ion cyclotron wave scattering.

Plain Language Summary The 1859 Carrington magnetic storm is the largest storm in recorded history. It is used as a model of an "extreme storm" by the U.S. Homeland Security for effects of such an event on the U.S. population. Computer modelers have tried to duplicate the magnetic ground signatures of the storm that were published in Tsurutani et al. (2003, https://doi.org/10.1029/2002JA009504). Some have used extremely high solar wind densities, values which have never been detected in the space age. Here we explain why assumptions of such high densities are unnecessary.

1. Results

We commend Ngwira and coauthors for their scholarly and excellent effort on modeling the Carrington 1859 magnetic storm. We have several comments, which, if adopted, may help improve modeling results. We hope that the authors will accept our comments in a positive light and redo their modeling in the near future.

2. Plasma Densities

High sheath solar wind densities of ~400 cm^{-3} have been assumed by Ngwira et al. (2014). Other researchers have assumed quite different values for the solar wind densities. The steady state solution of Manchester et al. (2006) predicts an unusually high slow solar wind density of 38 cm^{-3} at 1 AU. With a shock compression factor of about 4 times, their model produces a downstream sheath density of 146 cm^{-3}.

We believe that there is already evidence that plasma densities in the sheath sunward of (behind) the fast forward interplanetary shock were not particularly high, but lower than the above two assumed values. If we take an average solar wind density of ~5 cm^{-3} and a maximum compression ratio of ~4 as experimentally (Kennel, Edmiston, et al., 1984; Kennel, Scarf, et al., 1984; Tsurutani et al., 2008) and theoretically (Kennel, Edmiston, & Hada, 1985) shown for interplanetary space, we get a downstream sheath density of ~20 cm^{-3}. That taken with the Tsurutani et al. (2003) and Lakhina et al. (2012) derived solar wind speed of ~1,850 km s^{-1} at 1 AU gives a ram pressure of 114 nPa. This ram pressure can produce a Sudden Impulse (SI^+) of ~160 nT less ground induction effects (Araki et al., 1993; Siscoe et al., 1968; Tsurutani & Lakhina, 2014). Thus, the 120 nT SI^+ observed at the Colaba Observatory in 1859 extreme magnetic storm event (Tsurutani et al., 2003) is easily explained by more-or-less ordinary solar wind density values. It should be noted that a SI^+ value of 120 nT is high, but nowhere near the record value of ~202 nT for the 24 March 1991 shock event measured at Kakioka, Japan (Araki et al., 1997).

We note that the shock and sheath are not part of the interplanetary coronal mass ejection (ICME) (see Tsurutani et al., 2011), as some people have mistakenly stated in the literature. Although they are

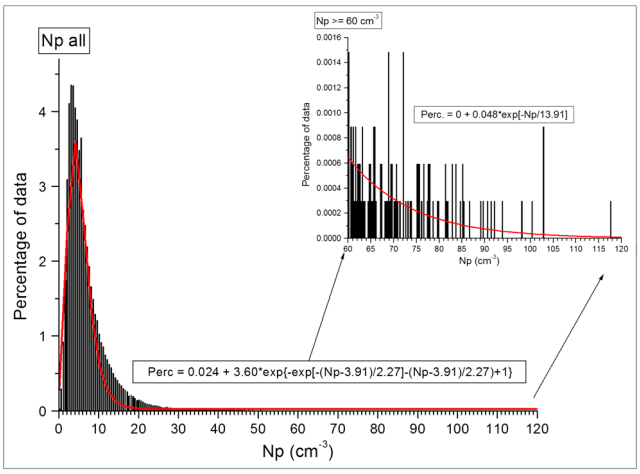

Figure 1. One-hour average solar wind densities from 1964 to 2017. The main part of the distribution is fitted with a skewed Gaussian function. The extreme values (>60 cm^{-3}) are blown up on the right-hand side. The latter is fitted with an exponential function.

physically located adjacent to the ICME proper, the plasma does not come from the same location of the Sun. The sheath is swept up and shocked (heated and compressed) slow solar wind plasma and magnetic fields. The solar and solar wind origins of the sheath plasma and magnetic fields are different from those of the ICME.

One part of the ICME, the magnetic cloud (Burlaga et al., 1981; Echer et al., 2008; Tsurutani et al., 1988), is characterized by low plasma beta ($\beta = 8\pi\ NkT/B^2$) values, where k is the Boltzmann constant, T is the plasma temperature, and B is the magnetic field magnitude. Thus, this region should not be a high plasma density region either.

If there are very high plasma densities, where would they be located? There is one part of an ICME, which is known to have very high plasma densities. This is the most sunward part, called the "filament" (see Illing & Hundhausen, 1986). In almost all cases, this part of the CME does not reach 1 AU (this is one reason why we use a different name for ejecta that reach 1 AU: "interplanetary CMEs" or ICMEs). Very few (~4%) filaments have been detected at Earth distances (Lepri & Zurbuchen, 2010). The first case of a filament was observed by the Wind spacecraft in the 10–11 January 1997 ICME event and reported by Burlaga et al. (1998). The filament had a peak density of ~164 cm^{-3} (several 5 min average values) and was located sunward of the magnetic cloud. This location is the standard position within a CME at the Sun, as indicated by Illing and Hundhausen (1986).

Li et al. (2006) had placed a high-density ~1,800 cm^{-3} plasma plug in the region sunward of the magnetic cloud to model a *Dst* ~1,600 nT Carrington magnetic storm. The authors placed such high densities behind the magnetic cloud to attempt to explain the short duration of the magnetic storm recovery phase. The high solar wind density produced consistency between an empirical model of *Dst* (Temerin & Li, 2002) and solar wind parameters. This location would imply that such a high-density plasma plug might be an ICME filament.

In order to address the question of how high solar wind densities can become, we have examined all available 1 h averages at 1 AU from 1964 to 2017, ~54 years. Figure 1 shows the distribution of these hourly average densities taken from the OMNI data site. In the right-hand side of the figure is an enlargement of the density events with values between 60 and 120 cm^{-3}. The peak density occurred on day 210, 1977 and was 118 cm^{-3}. This appears to be a sheath event.

The average density for the ~54 years was 6.8 cm^{-3}, a median of 5.2 cm^{-3}, and a standard deviation of 5.5 cm^{-3}. The peak in the histogram is at ~3.0 cm^{-3}. In our previous calculation, we used the median value. The reader should note that different solar wind features are known to have different densities. This figure includes high-speed streams, slow-speed streams, ICMEs, corotating interaction regions (CIRs), and the heliospheric current sheet.

The density main distribution has been fitted with a skewed Gaussian function. This was done because the value starts at zero and shows a tail distribution due to extreme values associated with ICMEs, sheaths, CIRs, and HPS. The central position of this fitted function is 3.9 cm^{-3}, which is closer to the median value rather than to the average value. The spread of this fitted function is 2.3 cm^{-3}, which is ~1/2 of the standard deviation of a normal Gaussian function. Note that the density functional curve fits well only around the peak, underestimating values between ~10 and 30 cm^{-3}, but overestimating the extreme tail for densities above 60 cm^{-3}.

For the extreme values, here taken as Np > 60 cm^{-3}, another exponential decay function has been fitted, with an exponential of $e^{-(n/13.9\ cm-3)}$, This extreme tail function could be used by modelers to identify the probability of the occurrence of extreme densities.

3. Magnetic Field Intensities

Figure 2 shows the OMNI 1 h average interplanetary magnetic field magnitude over the same time interval as in Figure 1, from 1964 to 2017. The average magnetic field magnitude is 6.3 nT, the median is

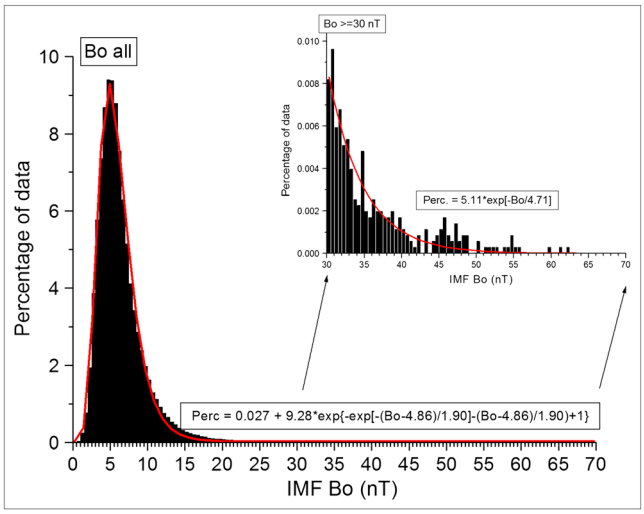

Figure 2. Same format as in Figure 1 but for the interplanetary magnetic field magnitude B_0. A blowup of the magnetic field between 30 nT and 70 nT is given in the inset.

5.6 nT, and the standard deviation is 3.2 nT. The maximum magnetic field was 62 nT and the minimum was 0.4 nT. The peak in the histogram is at 5.0 nT. We make the same caveats as for the plasma densities: the composition of these magnetic field values is a mixture of many different types of solar wind phenomena.

The entire magnetic field magnitude distribution has also been fitted with a skewed Gaussian function. The central position of this fitted function is 4.9 nT, which is closer to the median than to the average. The spread of this fitted function is 1.9 nT. The function fits the bulk of the distribution well, but underestimates the region between ~13 and 20 nT and overestimates the distribution for values >30 nT.

For magnetic field magnitude values >30 nT, an exponential decay fit has been made ($e^{-(B/-4.7\ nT)}$). This exponential decay can be used to calculate the probability of extreme magnetic field magnitude events.

We believe that the value of interplanetary magnetic field $B_z = -210$ nT considered by Ngwira et al. (2014) is too large and a bit unrealistic for the 1859 Carrington magnetic storm. Tsurutani et al. (2003) and Lakhina and Tsurutani (2017) have used the empirical relationship between the solar wind speed and the magnetic field intensity of the magnetic cloud at 1 AU (Gonzalez et al., 1998) to obtain the magnetic cloud magnetic field of ~90 nT for the Carrington storm. This leads to a maximum interplanetary electric field of ~160 mV m^{-1}. During the Carrington magnetic storm, the lowest latitude auroras were seen at 23° (Kimball, 1960). Using this latter information, the plasmapause location was determined to be at L = 1.3. This in turn was used to derive the magnetospheric convection electric field of ~20 mVm^{-1} (Tsurutani et al., 2003). Assuming a magnetic field reconnection efficiency of ~10%, this convection electric field corresponds to an interplanetary electric field of ~200 mVm^{-1}. Thus, these two estimates of the interplanetary electric field are in good agreement with each other. The resultant calculated magnetic storm intensity was $Dst = -1{,}760$ nT.

4. High Plasma Densities and Fast Storm Recovery Phases

It was noted by Li et al. (2006) that the Carrington magnetic storm recovery phase was quite rapid, thus the inclusion of a high-density plasma plug sunward of the magnetic cloud in their model. Here we postulate a new idea for rapid storm recovery phases during extremely intense magnetic storms.

The magnetic storm intensity is related to the magnetospheric convection electric fields (Gonzalez et al., 1989). The larger the convection electric field, the deeper the midnight sector penetration of the plasmasheet ions and electrons toward the Earth. Assuming conservation of the particle adiabatic invariants, the ring current particles gain more kinetic energy, leading to the observed larger negative *Dst* values (large storm intensities).

Besides the higher ring current particle energies, there are several other important aspects of the convection of energetic plasma to low L regions of the magnetosphere that are typically not considered. First, the extreme compression of the particles in perpendicular temperature (conservation of the first adiabatic invariant) will lead to greater free energy for the loss cone instability (Kennel & Petschek, 1966; Tsurutani & Lakhina, 1997). Additionally at lower L the loss cone size is substantially larger. Thus, for both of these reasons, we suspect that the wave intensities (both proton electromagnetic ion cyclotron waves and electron electromagnetic (chorus) waves) will be substantially greater for extreme magnetic storms. This can be tested by wave measurements during magnetic storms of lesser intensities and theoretical modeling. Second, because of the greater loss cone size and the greater wave intensities, rapid ring current losses can be expected. The more intense the storm, the faster the ring current loss rate. Wave coherency (Tsurutani et al., 2009, 2013; Lakhina et al., 2010; Bellan, 2013; Remya et al., 2015) in wave-particle cyclotron resonant interactions should be considered in any updated model.

In the above, we have focused on wave-particle interactions for the loss of extreme storm ring current particles. However, it is noted that other (standard) loss processes (Jordanova et al., 1998; Kozyra et al., 2006) will

also be in effect for extreme magnetic storm cases. Coulomb collisions and charge exchange processes may be substantially higher for low L-shell ring currents. Theoretical comparisons should be made to determine the relative losses associated with the different mechanisms.

5. Final Comments

Our hope is that Ngwira et al. and other magnetic storm modelers will try to include some of these parameters to model the Carrington magnetic storm. So far, a variety of parameters have been assumed and used, with only mixed results so far. We have made arguments why high plasma densities either in the sheath, the ICME magnetic cloud, or trailing ICME filament are not needed to explain the Carrington event features. However, it should be recognized that ring current particle losses are nonlinear (increasing rate of loss with increasing storm intensity), and not just a constant factor. We hope modeling with the numbers given in this comment will allow a better match between models and observations.

Acknowledgments
Portions of this research were done at the Jet Propulsion Laboratory, California Institute of Technology, under contract with NASA. R.H. would like to thank ANR for financial support through the financial agreement ANR-15-CE31-0009-01 at LPC2E/CNRS and CNES for postdoctoral fellowship support at LPC2E/CNRS. G.S. L. thanks the National Academy of Sciences, India, for support under the NASI-Senior Scientist Platinum Jubilee Fellowship Scheme. E. E. wishes to acknowledge Brazilian agency CNPq/PQ302583/2015-7 for financial support for this work.

References

Araki, T., Fujitani, S., Emoto, M., Yumoto, K., Shiokawa, K., Ichionose, T., … Liu, C. F. (1997). Anomalous sudden commencement on March 24, 1991. *Journal of Geophysical Research*, *102*, 14,075–14,086.

Araki, T., Funato, K., Iguchi, T., & Kamei, T. (1993). Direct detection of solar wind dynamic pressure effect on ground geomagnetic field. *Geophysical Research Letters*, *20*, 775–778. https://doi.org/10.1029/93GL00852

Bellan, P. M. (2013). Pitch angle scattering of an energetic magnetized particle by a circularly polarizec electromagnetic wave. *Physics of Plasmas*, *20*(4), 042117. https://doi.org/10.1063/1.4801055

Burlaga, L., Fitzenreiter, R., Lepping, R., Olgilvie, K., Szabo, A., Lazarus, A., … Larson, D. E. (1998). A magnetic cloud containing prominence material: January 1997. *Journal of Geophysical Research*, *103*, 277–285. https://doi.org/10.1029/97JA02768

Burlaga, L., Sittler, E., Mariani, F., & Schwenn, R. (1981). Magnetic loop behind an interplanetary shock: Voyager, Helios, and IMP 8 observations. *Journal of Geophysical Research*, *86*, 6673–6684. https://doi.org/10.1029/JA086iA08p06673

Echer, E., Gonzalez, W. D., Tsurutani, B. T., & Gonzalez, A. L. C. (2008). Interplanetary conditions causing intense geomagnetic storms ($Dst \leq -100$ nT) during solar cycle 23 (1996-2006). *Journal of Geophysical Research*, *113*, A05221. https://doi.org/10.1029/2007JA012744

Gonzalez, W. D., Clua de Gonzalez, A. L., Dal Lago, A., Tsurutani, B. T., Arballo, J. K., Lakhina, G. S., … Ho, C. M. (1998). Magnetic cloud field intensities and solar wind velocities. *Geophysical Research Letters*, *25*, 963–966. https://doi.org/10.1029/98GL00703

Gonzalez, W. D., Tsurutani, B. T., Gonzalez, A. L. C., Smith, E. J., Tang, F., & Akasofu, S.-I. (1989). Solar wind-magnetosphere coupling during intense magnetic storms. *Journal of Geophysical Research*, *94*, 8835–8851. https://doi.org/10.1029/JA094iA07p08835

Illing, R. M. E., & Hundhausen, A. J. (1986). Disruption of a coronal streamer by an eruptive prominence and coronal mass ejection. *Journal of Geophysical Research*, *91*, 10,951–10,960. https://doi.org/10.1029/JA091iA10p10951

Jordanova, V. K., Farrugia, C. J., Janoo, L., Quinn, J. M., Torbert, R. B., Ogilvie, K. W., … Belian, R. D. (1998). October 1995 magnetic cloud and accompanying storm activity: Ring current evolution. *Journal of Geophysical Research*, *103*, 79–92. https://doi.org/10.1029/97JA02367

Kennel, C. F., Edmiston, J. P., & Hada, T. (1985). A quarter century of collisionless shock research. In *Collisionless shocks in the heliosphere: A tutorial review*, *Geophysical Monograph Series* (Vol. 34, p. 1). Washington DC: American Geophysical Union.

Kennel, C. F., Edmiston, J. P., Scarf, F. L., Coroniti, F. V., Russell, C. T., Smith, E. J., … Temerin, M. (1984). Structure of the November 12, 1978, quasi-parallel interplanetary shock. *Journal of Geophysical Research*, *89*, 5436–5452. https://doi.org/10.1029/JA089iA07p05436

Kennel, C. F., & Petschek, H. E. (1966). Limits on stably trapped particle fluxes. *Journal of Geophysical Research*, *71*, 1–28. https://doi.org/10.1029/JZ071i001p00001

Kennel, C. F., Scarf, F. L., Coroniti, F. V., Russell, C. T., Wenzel, K.-P., Sanderson, T. R., … Scholer, M. (1984). Plasma and energetic particle structure upstream of a quasi-parallel interplanetary shock. *Journal of Geophysical Research*, *89*, 5419–5435. https://doi.org/10.1029/JA089iA07p05419

Kimball, D. S. (1960). A study of the aurora of 1859, Sci. Rpt. 6, UAG-R109, University of Alaska, Fairbanks AK.

Kozyra, J. U., Nagy, A. F., & Slater, D. W. (2006). High-altitude energy source(s) for stable auroral red arcs. *Reviews of Geophysics*, *35*, 155–190.

Lakhina, G. S., Alex, S., Tsurutani, B. T., & Gonzalez, W. D. (2012). Supermagnetic storms: Hazard to society. In A. S. Sharma, et al. (Eds.), *Extreme events and natural hazards: The complexity perspective*, *Geophysical Monograph Series* (Vol. 196, p. 267). Washington D.C: American Geophysical Union. https://doi.org/10.1029/2011GM001073

Lakhina, G. S., & Tsurutani, B. T. (2017). Super geomagnetic storms: Past, present and future, to appear. In N. Buzulukova (Ed.), *Extreme geospace* (Chap. 7, p. 157.). Cambridge: Cambridge University Press.

Lakhina, G. S., Tsurutani, B. T., Verkhoglyadova, O. P., & Pickett, J. S. (2010). Pitch angle transport of electrons due to cyclotron interactions with the coherent chorus subelements. *Journal of Geophysical Research*, *115*, A00F15. https://doi.org/10.1029/2009JA014885

Lepri, S. T., & Zurbuchen, T. H. (2010). Direct observational evidence of filament material within interplanetary coronal mass ejections. *Astrophysical Journal Letters*, *723*(1), L22–L27. https://doi.org/10.1088/2041-8205/723/1/L22

Li, X., Temerin, M., Tsurutani, B. T., & Alex, S. (2006). Modeling of 1–2 September 1859 super magnetic storm. *Advances in Space Research*, *38*(2), 273–279. https://doi.org/10.1016/jasr.2005.06.070

Manchester, W. B. IV, Ridley, A. J., Gombosi, T. I., & DeZeeuw, D. L. (2006). Modeling the Sun-to-Earth propagation of a very fast CME. *Advances in Space Research*, *38*(2), 253–262. https://doi.org/10.1016/j.asr.2005.09.044

Ngwira, C. M., Pulkkinen, A., Kuznetsova, M. M., & Glocer, A. (2014). Modeling extreme "Carrington-type" space weather events using three-dimensional global MHD simulations. *Journal of Geophysical Research: Space Physics*, *119*, 4456–4474. https://doi.org/10.1002/2013JA019661

Remya, B., Tsurutani, B. T., Reddy, R. V., Lakhina, G. S., & Hajra, R. (2015). Electromagnetic cyclotron waves in the dayside subsolar outer magnetosphere generated by enhanced solar wind pressure: EMIC wave coherency. *Journal of Geophysical Research: Space Physics*, *120*, 7536–7551. https://doi.org/10.1002/2015JA021327

Siscoe, G. L., Formisano, V., & Lazarus, A. J. (1968). Relation between geomagnetic sudden impulses and solar wind pressure changes-an experimental investigation. *Journal of Geophysical Research*, *73*, 4869–4874. https://doi.org/10.1029/JA073i015p04869

Temerin, M., & Li, X. (2002). A new model for the prediction of *Dst* on the basis of the solar wind. *Journal of Geophysical Research*, *107*(A12), 1472. https://doi.org/10.1029/2001JA007532

Tsurutani, B. T., Echer, E., Guarnieri, F. L., & Kozyra, J. U. (2008). CAWSES November 7–8 2004, superstorm: Complex solar and interplanetary features in the post-solar maximum phase. *Geophysical Research Letters*, *35*, L06S05. https://doi.org/10.1029/2007GL031473

Tsurutani, B. T., Gonzalez, W. D., Lakhina, G. S., & Alex, S. (2003). The extreme magnetic storm of 1–2 September 1859. *Journal of Geophysical Research*, *108*(A7), 1268. https://doi.org/10.1029/2002JA009504

Tsurutani, B. T., Gonzalez, W. D., Tang, F., Akasofu, S.-I., & Smith, E. J. (1988). Origin of interplanetary southward magnetic fields responsible for major magnetic storms near solar maximum (1978-1979). *Journal of Geophysical Research*, *93*, 8519–8531. https://doi.org/10.1029/JA093iA08p08519

Tsurutani, B. T., & Lakhina, G. S. (1997). Some basic concepts of wave-particle interactions in collisionless plasmas. *Reviews of Geophysics*, *35*, 491–501. https://doi.org/10.1029/97RG02200

Tsurutani, B. T., & Lakhina, G. S. (2014). An extreme coronal mass ejection and consequences for the magnetosphere and Earth. *Geophysical Research Letters*, *41*, 287–292. https://doi.org/10.1002/2013GL058825

Tsurutani, B. T., Lakhina, G. S., & Verkhoglyadova, O. P. (2013). Energetic electron (>10 keV) microburst precipitation, ~5–15s X-ray pulsations, chorus, and wave-particle interactions: A review. *Journal of Geophysical Research: Space Physics*, *118*, 2296–2312. https://doi.org/10.1002/jgra.50264

Tsurutani, B. T., Lakhina, G. S., Verkhoglyadova, O. P., Gonzalez, W. D., Echer, E., & Guarnieri, F. L. (2011). A review of interplanetary discontinuities and their geomagnetic effects. *Journal of Atmospheric and Solar - Terrestrial Physics*, *73*(1), 5–19. https://doi.org/10.1016/j.jastp.2010.04.001

Tsurutani, B. T., Verkhoglyadova, O. P., Lakhina, G. S., & Yagitani, S. (2009). Properties of dayside outer zone chorus during HILDCAA events: Loss of energetic electrons. *Journal of Geophysical Research*, *114*, A03207. https://doi.org/10.1029/2008JA013353